MECHANICAL BEHAVIOR ANALYSIS OF THE AUTOMOTIVE PARTS JOINTS MADE THROUGH RESISTANCE SPOT WELDING

Gheorghe Bogdan PULPEA[1]*, Mihai Alexandru STĂNOIU[2], Adrian ROTARIU[3], Ionelia VOICULESCU[4], Andreea MOLDOVAN[5], Daniela PULPEA[6]

Resistance spot welding (RSW) is a common method of connecting metallic sheets in the automotive industry. For optimizing welding settings and reducing weld failure under normal conditions of handling, storage, and use of metallic automotive structures, destructive tests (using both qualitative and quantitative approaches) are required. Calculations and particular testing are used to determine RSW's parameters and circumstances. This research examines the welding characteristics of auto parts comprised of two sheets of carbon steel joined by multiple resistance spot welding in real structures design. Destructive control tests, which are commonly used to establish RSW properties, were conducted on predetermined-size samples that were destroyed during the experiments. This report describes the work done to evaluate the welding behaviour of these materials using three different types of tests: chisel, peel, and tensile–shear. The major goal of this research is to test the weld in real-world manufacturing settings in order to achieve the specified joint quality. The resistance to diverse stresses of these industrial metal components of automobiles is noticed through testing, with high load values of 31 kN obtained, as well as the breaking mode that corresponds to the theoretical circumstances imposed.

Keywords: spot welding, part joints, nugget,

1. Introduction

Resistance spot welding (RSW) is a common essential procedure used in automotive manufacturing industry [1-3] that can be applied to solid structures and to small metal sheet parts with excellent benefits [4-5]. To ensure a good quality of the spot welds it is required to control the input welding parameters [1]. Quantitative experiments have been used to demonstrate the importance of welding current and

[1] Lecturer, PhD Eng., Military Technical Academy, 39-49 George Coșbuc Blvd., 050141, Bucharest, Romania, pulpea.b@gmail.com; *corresponding author.
[2] Eng., University POLITEHNICA of Bucharest, 313 Splaiul Indepedentei, 060042, Bucharest, Romania, mihai.stanoiu30@yahoo.com.
[3] Professor, PhD Eng., Military Technical Academy, 39-49 George Coșbuc Blvd., 050141, Bucharest, Romania, adrian.rotariu@mta.ro.
[4] Professor, PhD Eng., University POLITEHNICA of Bucharest, 313 Splaiul Indepedentei, 060042, Bucharest, Romania, ioneliav@yahoo.co.uk.
[5] Lecturer, PhD Eng., Military Technical Academy, 39-49 George Coșbuc Blvd., 050141, Bucharest, Romania, andreea.moldovan@mta.ro.
[6] Scientific Researcher, PhD Eng., Military Technical Academy, 39-49 George Coșbuc Blvd., 050141, Bucharest, Romania, daniela.pulpea@mta.ro.

duration values in the resistance spot welding process [4], [6-8] of automotive steel sheets samples. A computer-controlled robotic welder, an industrial spot-welding machine, or a portable hand spot welder can all perform the RSW procedure. Theoretical estimations of welding parameters, operator skills, and technician expertise have not always been precise or correct, nor have they always corresponded to the ideal process characteristics [8-9]. The correct adjustment of every parameter for each welding equipment has always been difficult due to all the sensitive aspects involved. As a result, many specimens of the construction material must be evaluated to achieve ideal values for the welding input parameters, resulting in an increase in production costs.

Pouranvari et al. [10] provide an analytical model to predict spot welding failure in a research study. Theoretical approaches based on mathematical calculus methods, as well as spot-welded joints using three-dimensional finite element models [2], [11], play an important role in the design stages of welded structures, representing preliminary input values for the apparatus and reducing the number of destructive tests performed. However, in order to anticipate and analyze the possibility of weld failure more precisely, the metallurgical features of the welds must be taken into account. A wide range of destructive and non-destructive techniques were created to carry out the type of mechanical tests. [1], [6-7], [12-14]. To guarantee the safety and quality of the products, visual examination is carried out in accordance with the product control plan during qualitative inspection and evaluation of physical characteristics of weld spots throughout automotive production. [15-16]. This verification focuses on the presence of welding points, the quality of the surface interaction, and other aspects that can be visually detected (the spot alignment, scratched or hit parts, material expulsions, sizing of welding interface diameters, etc.). To obtain optimal results it is necessary that the sheets do not have on the surfaces any organic compounds or other substances that can induce a high contact resistance and be free of burrs (burrs can cause shunting effects). This visual evaluation can also be done with specialized equipment and software that selects only the compliant parts based on a precise image analysis. Welding process monitoring and control involves routine or continuous monitoring of the process variable parameters. The mechanical tests described in all research papers [9-13] are usually performed on standard dimensioned strip-type samples [17-19], [20] in precisely conditions of welding in accordance with EN ISO 5182:2016 [21] at one or more collinear points by changing welding current and welding time.

This research examined the behaviour of spot-welded steel sheets, generated from actual automobile parts, through destructive quantitative and qualitative studies. The major objective was to investigate the weld in actual manufacturing settings in order to achieve the necessary joint quality.

2. Experimental studies

The steel sheets were welded using an RSW industrial machine with a capacity of 75KVA-250KVA by changing the electrode form, materials type, cooling water flow rate, and electrode force. This study examines the behaviour of small, real-world welded automotive components under laboratory conditions using visual examination (VE), failure mode analyses (FMA), dimensional analysis (DA), tensile-shear test (TS), and manual destructive test (simple test - ST) methods like the chisel test and peel test.

2.1. Materials

The parts studied are real industrial steel-sheets comprising multiple welded spots with different thicknesses and geometries, which are used in different attachments, components of vehicles bodies, provided by S.C. SILDVB COM S.A Company from Romania. In Table 1 are presented the main parts with welding parameters and physic characteristics. The steel sheet used is DC04 DIN EN-10130 with chemical composition Fe-0.08C-0.03P-0.4Mn-0.03S and mechanical proprieties of 210-215 MPa yield strength, 270-350 MPa tensile strength and 38% elongation. To achieve the test program investigation the parts needed some transformation steps presented in Fig.1.

Table 1

Main parts and weld joint characteristics

No.	Parts	Sheets	Weld characteristics			Steel-sheets characteristics			Tests
			I (A)	F (daN)	T.S (cycle)	Weld Spot no.	Weight (g)	Thickness (mm)	
1	**A.01**	R.01.1 R.01.2	16	1050	7	3	455	2.03 2.45	VE TS
2	**A.02**	R.02.1 R.02.2	15.5	1010	7	3	454	2.00 2.46	VE ST/ TS
3	**A.03**	R.03.1 R.03.2 R.03.3	7.5	290	7	2 4	312	2.51 2.52 1.50	VE TS ST
4	**A.04**	R.04.1 R.04.2 R.04.3	7.5	290	7	2 4	313	2.54 2.53 1.52	VE TS ST
5	**A.05**	R.05.1 R.05.2	17	750	7	2	332	2.56 2.56	VE TS
6	**A.06**	R.06.1 R.06.2	9.5	220	10.5	2	152	1.54 1.51	VE ST

The samples were prepared by cutting the metal structures indicated with red line in Fig. 1 at a workstation provided with a heavy-duty bench vise, an angle grinder, pliers, stone bench grinder, hydraulic press, and goggles for protection. The cutting parts were done by holding the parts one by one in the bench vise

using the angle grinder, and the resulted sharp edge was clear by a 45 degrees chamfer.

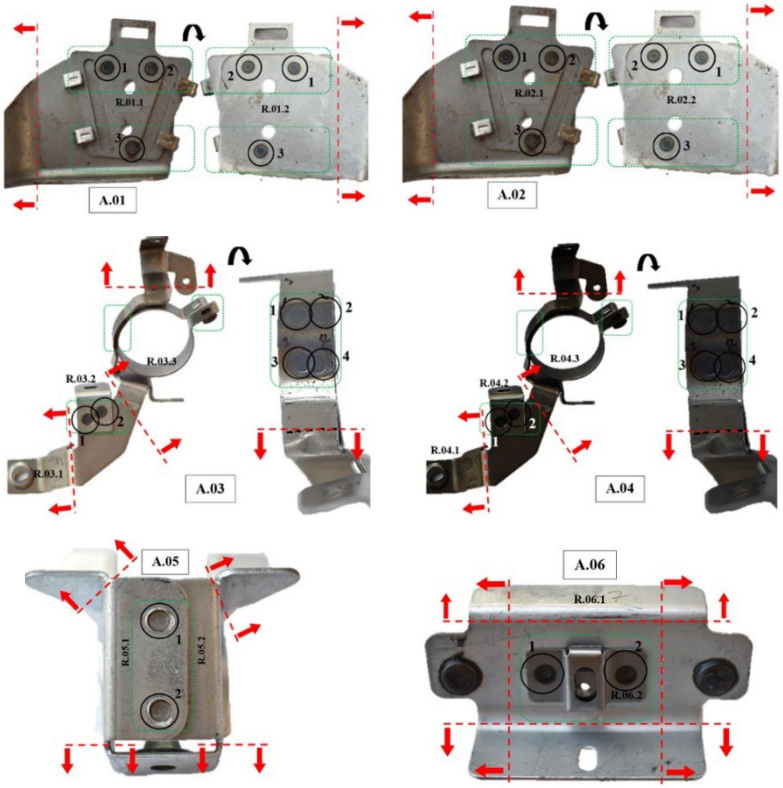

Fig. 1. Steel samples [16] (red line – cutting areas; green rectangular – weld spot zone)

The curved areas of the cut parts were carefully directed, in order to create the fixing zone in the mechanical clamping. After the cutting process, the resulted samples are represented in Fig.4 and were analysed as follow: from A.01 to SA.01; from A.02 to SA.02; from A.03 to SA.03.1 and SA.03.2; from A.04 to SA.04.1 and SA.04.2; from A.05 to SA.05; from A.06 to SA.06.

2.2. Methods

The testing program has been carried out using the following methods: visual examination (VE); simple test (ST) by manual destruction (chisel and peel tests); mechanical tests by tensile-shear test (TS).

In the RSW process, after a certain time, a molten metal core belonging to both steel-sheets was formed in the pressure area. The core had increased in size while the electric welding resistance was active. When this process had ended, the molten core has solidified. As a result, the welding point on the surface of both sheets was formed. In a cross-section, made in the welded joint zone, the geometry of the nugget can be observed by metallographic analysis, as is represented in Fig.2. The nugget dimension was given by the weld size in terms of nugget width or

diameter. Based on the weld nugget geometry, during the visual examination of the samples, the weld aspect appreciation and spot surface measuring (include only HAZ - heat affected zone, de - indentation width of bottom sheet, e1- indentation depth of bottom sheet) was performed.

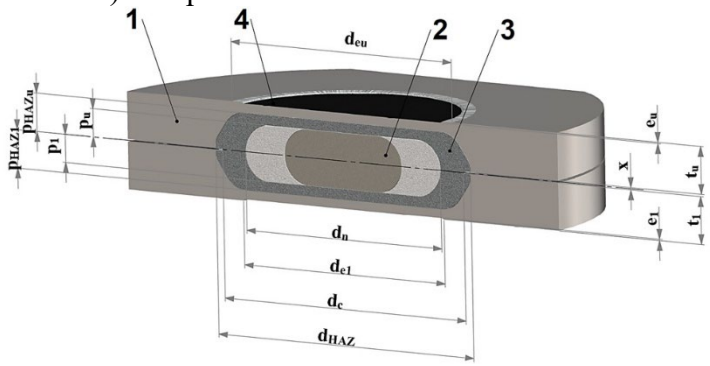

Fig. 2. Geometry and dimensions of the weld nugget [15]
Legend: 1 – sheet, 2 – core/fusion zone (FZ), 3 — heat affected zone (HAZ), 4 – electrode trace, dc – weld width, de1 – indentation width of bottom sheet, deu – indentation width of up sheet, dHAZ – HAZ width, dn – nugget width, e1 – indentation depth of bottom sheet, eu – indentation depth of up sheet, p1 – nugget depth in bottom sheet, pu – nugget depth in up sheet, t1 – bottom sheet thickness, tu – up sheet thickness, x – sheets gap.

The simple test included the following procedures: “chisel test” and “peel test” [16-18]. These are the most used methods and require a minimum necessary equipment. They include visual analyses of the failure mode and dimensional analysis of nugget or interfacial characteristics, but they can be used only for qualitative control. The advantage is that the welding parameters can be verified in real time during the industrial technological flow. For the peel test, the welds were tested by fixing one of the samples in a bench vise. By means of a tool, either pliers or a special notched tool, a force was applied for inducing in the welded spot a load (axial tension) perpendicular to the welding surface, until welding failure. For the destructive chisel test, a chisel was inserted between the zones that separate the sheets while the weld was loaded perpendicular to the surface. The chisel may have one or two blades separated by a notch and the force was applied manually by striking with a hammer.

The welded components were subjected to a tensile-shear test (TS) in a laboratory setting using a TC-100 computer control electronic universal testing equipment (precision of deformation: 0.5 percent; adjustment range of displacement rate: 0.01-500mm/min; discrimination of displacement: 0.001 mm). The tensile speed was held constant throughout the test. The tensile-shear strength findings were calculated using load-elongation diagrams with the maximum breaking force. The following parameters can be retrieved from the load–displacement curve to fully explain the mechanical behaviour of a spot weld [13]: P_{max} stands for peak load; L_{max} stands for elongation at peak load (a measure of joint ductility); and W_{max} stands for failure energy at peak load (a measure of weld energy

absorption capabilities), while a higher value can indicate improved weld performance against impact loads, such as accidents.

Fig. 3 shows a schematic representation of weld surface flaws at the main failure modes that can be observed during mechanical testing. Spot welds can fail in four different ways, depending on the thickness of the steel sheets and the weld strength test [13], [17]: interfacial failure (IF) – shearing the welding point, compromising vehicle crashworthiness; pull-out failure (PF)/button failure/plug failure – forming a weld nugget (button) from a single sheet with the best mechanical properties; partial interfacial mode (PIF) – partial plug failure; partial thickness – partial pull-out (PT-PP).

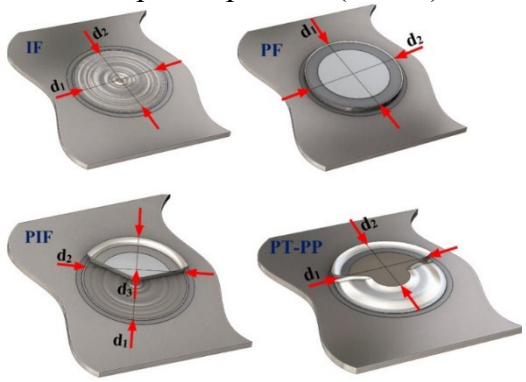

Fig. 3. Various failure types that can occur during RSW mechanical testing described schematically

$$\textbf{(IF)} \quad d = d_n = d_1 \approx d_2 \tag{1}$$

$$\textbf{(PF)} \quad d = d_p = \frac{(d_1 + d_2)}{2} \tag{2}$$

$$\textbf{(PIF)} \quad d_p = \frac{(d_2 + d_3)}{2} \tag{3}$$

$$d = \frac{(d_1 + d2)}{2} \tag{4}$$

$$\textbf{(PT-PP)} \quad d = \frac{(d_1 + d_2)}{2} \tag{5}$$

where: d – average weld diameter (mm)
d_p – plug diameter (mm)
d_n – nugget diameter (mm)
d_1 – largest weld dimension (mm)
d_2 – small weld dimension (mm)

The dimensional analysis of RSW fracture [18-19] can be made using the equations 1 to5. The nugget size was measured using a digital caliper Mitutoyo ABSOLUTE Digimatic caliper model, series 500 with a measuring accuracy of 0.02 mm and used in weld quality evaluation. An acceptable weld has a nugget width greater or equal to the minimum weld size as shown in Table 2 [22].

Table 2

Minimum acceptable weld size [20]

Sheets Thickness (mm)	Weld Size (mm)	Sheets Thickness (mm)	Weld Size (mm)	Sheets Thickness (mm)	Weld Size (mm)
0.60-0.79	3.5	1.30-1.59	5.0	2.30-2.69	6.5
0.80-0.99	4.0	1.60-1.89	5.5	2.70-3.09	7.0
1.00-1.29	4.5	1.90-2.69	6.0	3.10-3.59	7.5

3. Results and discussions

The visual examination (Fig. 4) of welding spot (WS) dimensions, was performed using a digital caliper. The measurement results are presented in Table 3 and Table 4.

Fig. 4. Surfaces of welded points

The samples present two or more welding spots with different spot distances, depending on the free space of the sample. On the steel-sheet surface, the joints showed a good aspect with all the required characteristics. The thermal zone for the samples SA 04.01 and SA 04.2 is not visible and could not be measured, because some of the sheets were painted.

Table 3

Welded spot dimension for samples SA.01, SA.02, SA.03.1, SA.04.1, SA.05

Dimension	SA.01			SA.02			SA.03.1		SA.04.1*		SA.05	
	WS1	WS2	WS3	WS1	WS2	WS3	WS1	WS2	WS1	WS2	WS1	WS2
d_{HAZ} (mm)	9.22	9.44	9.88	9.47	9.39	9.48	9.40	9.53	N/A	N/A	9.33	9.33
d_e (mm)	6.05	5.65	5.88	6.61	6.52	6.61	6.59	6.40	5.21	6.65	7.70	7.71
e_1 (mm)	0.11	0.15	0.12	0.13	0.10	0.12	0.20	0.15	N/A	N/A	0.45	0.50
Spot** distance (mm)	(1-2)	30.99		(1-2)	25.88		(1-2)	13.52	(1-2)	10.95	(1-2)	32.09
	(1-3)	58.57		(1-3)	53.24							
	(2-3)	57.17		(2-3)	58.05							

* It is covered with paint and the thermally affected area cannot be seen;
** Spot distance between Welding Spot – WS (WS1, WS2, WS3, WS4) of each sample

Table 4

Welded spot dimension for samples SA.03.2, SA.04.2, SA.06

Dimension	SA.03.2				SA.04.2*				SA.06	
	WS1	WS2	WS3	WS4	WS1	WS2	WS3	WS4	WS1	WS2
d_{HAZ} (mm)	10.77	10.94	8.85	8.85	N/A	N/A	N/A	N/A	7.97	8.28
d_e (mm)	6.50	5.70	5.89	4.15	6.57	5.82	5.80	5.66	6.37	6.38
e_1 (mm)	0.25	0.20	0.25	0.20	0.1	0.1	0.1	0.1	0.09	0.06
	(1-2)	8.14			(1-2)	5.61			(1-2)	30.45
	(1-3)	16.29			(1-3)	15.84				

Spot ** distance (mm)	(2-4)	17.14	(2-4)	16.63		
	(3-4)	5.27	(3-4)	5.88		
* It is covered with paint and the thermally affected area cannot be seen ** Spot distance between Welding Spot – WS (WS1, WS2, WS3, WS4) of each sample						

All samples demonstrated interfacial failure (nugget separation) as a failure mode in the evaluation of the tested sample thicknesses (> 2.2 mm) using tensile-shear tests. As seen in Fig.5-7, the welded region at the interface of the two sheets yielded, leaving half of the nugget in one sheet and half in the other. This failure mode is explained by the fact that tensile loading in the sheet interface is below the shear loading in the weld interface and by the fact that the resistance of a material to shear force is about half of its resistance to normal force. The interface separation is also due to the high value of the sheet thickness in relation to the nugget width.

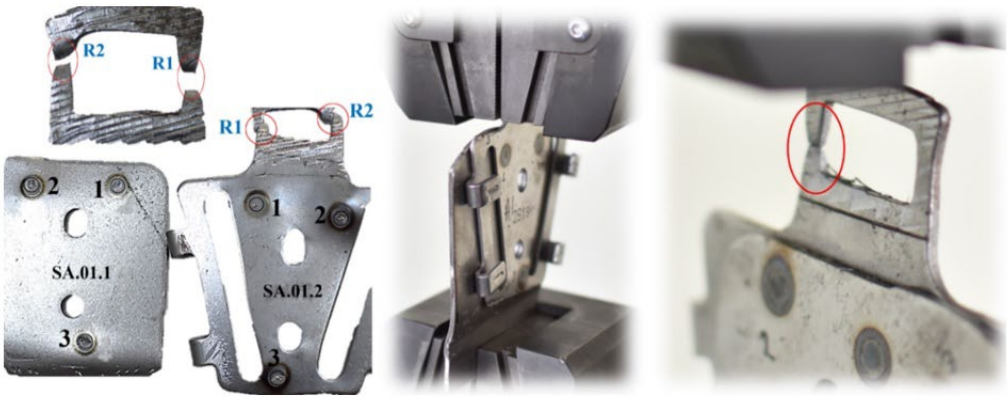

Fig. 5. Interfacial failure for sample SA.01

The data value for each welded spot of the samples are presented in Table 5. Because the interfacial fracture is asymmetrical, relation (4) was used for nugget diameter value. It is noticed that the tested samples followed the same pattern with different peak loads. The breaking mode for two or three welds observed in graphs (Fig. 8-11), consisted of increasing the maximum load until the nugget failure of the first welded spot (WS), was observed on the first stage and continues on the second stage at a lower force, remaining approximately constant until the final failure. The last two joints failed simultaneously in the case of the sample SA.01 that contains three welding spots in the second level.

Fig. 6. Interfacial failure for samples SA.03.1 and SA.04.1

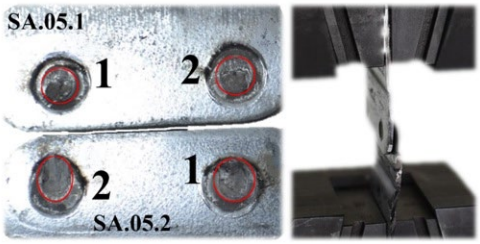

Fig. 7. Interfacial failure for sample SA.05

Table 5

Measurement of weld size for welds with interfacial failure

No.	Sample	Sheet	WS	d_{n1} (mm)	d_{n2} (mm)	d (mm)	Yielded spot	P_{max} (kN)
1	**SA.01**	SA.01.1	1	3.99	3.89	3.94	First	31.69
			2	4.75	4.04	4.39	Second	
			3	5.02	4.71	4.86	Second	
		SA.01.2	1	4.33	4.25	4.29	First	
			2	5.10	5.08	5.09	Second	
			3	4.63	4.57	4.60	Second	
2	**SA.03.1**	SA.03.1.1	1	4.92	3.80	4.36	First	17.09
			2	2.10	2.04	2.07	Second	
		SA.03.1.2	1	4.98	4.31	4.65	First	
			2	3.17	2.81	2.99	Second	
3	**SA.04.1**	SA.04.1.1	1	6.05	5.46	5.75	First	8.19
			2	3.10	2.48	2.79	Second	
		SA.04.1.2	1	5.36	4.99	5.17	First	
			2	3.71	3.28	3.49	Second	
4	**SA.05**	SA.05.1	1	6.28	5.44	5.86	Second	26.10
			2	6.59	6.01	6.30	First	
		SA.05.2	1	6.37	5.45	5.91	Second	
			2	6.16	5.98	6.07	First	

Aside from interface failure (the most disagreeable failure mode), the samples exhibit a high load capacity, with maximum forces surpassing 30 kN reported for the samples with three welding spots (Fig.8). The analyses of the

obtained parameters were performed in correlation with the breaking order of the welded spots. The parameters values obtained thru load-displacement diagrams are presented in Table 6.

Table 6

Parameters extracted from load–displacement curve

No.	Sample	First stage			Second stage			Sheet Failure	
		P_{max} (kN)	L_{max} (mm)	W_{max}	P_{max} (kN)	L_{max} (mm)	W_{max}	R1 F_{max} (kN)	R2 F_{max} (kN)
1	**SA.01**	31.69	0.85	18.54	22.30	0.51	9.15	11.64	16.13
2	**SA.03.1**	17.09	0.54	5.72	13.68	0.25	2.7	N/A	N/A
3	**SA.04.1**	8.19	0.70	2.90	4.10	0.23	0.48	N/A	N/A
4	**SA.05**	26.10	1.39	15.88	10.11	N/A	N/A	N/A	N/A
5	**SA.02**	N/A	N/A	N/A	N/A	N/A	N/A	24.72	14.63

The weld energy absorption capability was assessed based on the failure energy W_{max} values at peak load, a variable that influences the increase in weld performance dependability against impact loads and functionality.

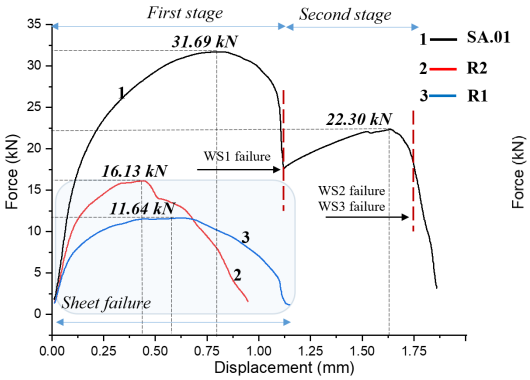

Fig.8. TS test showing the load-displacement diagram for SA.01 sample

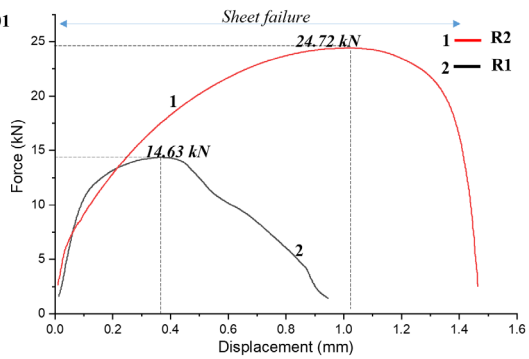

Fig. 9. TS test showing the load-displacement diagram for SA.02 sample

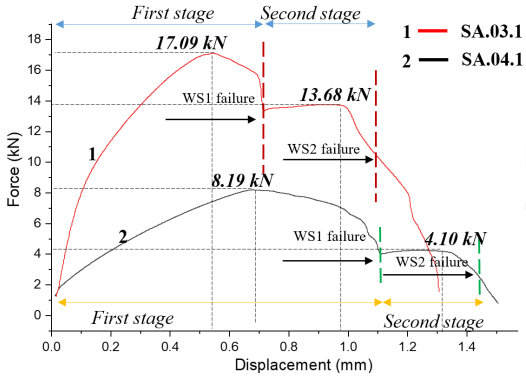

Fig. 10. TS test showing the load-displacement diagram for SA.03.1 and SA.04.1 samples

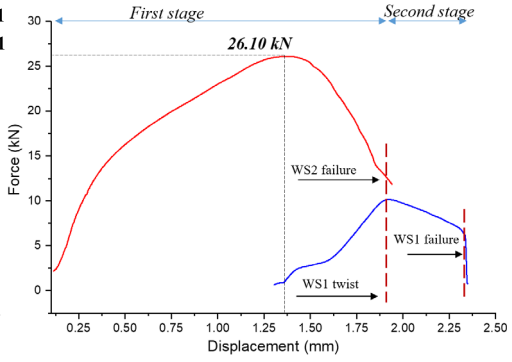

Fig. 11. TS test showing the load-displacement diagram for SA.05 sample

Although the samples SA.03.1 and SA.04.1(Fig.10) are similar joints tested with the same weld parameters, the tensile strength values were totally different. A simple change of parameters can substantial influence the welding strength. In the case of the samples SA.01 and SA.02 (Fig.8-9), the failure has located on clamping surface of steel sheet of R1 and R2 zones (Fig.5), where the thickness decrease. That can be justified by the fact that axial-tension in the steel-sheet was greater than tensile-shear in the weld spot. The behaviour of R1 and R2 zone under axial force are highlighted in Fig.8. Because the welded spot had not failed at that moment, the sample SA.01 was fixed and the test was reloaded obtaining the diagram presented in Fig.8 with two successive failures.

The sample SA.01 with three welded spots had the highest load value in both stages, with a similar profile with samples SA.03.1 and SA.04.1. After the nugget failure of WS1 in the first stage, in the second stage both WS2 and WS3 failed simultaneously (Figure 8). For the sample SA.02, it was the same evolution as for SA.01 sample, the tensile strength behaviour of R2 and R1 zones being illustrated in Fig.9, without the re-testing stage. The sample SA.02 has been also subjected to simple test (chisel test). For sample SA.05 (Fig.11) the evolution of the graph is explained by the fact that, during WS2 failure, the top sheet has rotated around the welding spot WS1, due to the location distance of the welding point comparatively with the axis of the testing system. This sample had the highest value of the welding point diameter and also a large load capacity with only two welded spots. Therefore, samples SA.01 and SA.05 had the greatest welding parameters values (I, F - Table 1) and provided the highest mechanical loads during tensile-shear test.

Fig. 12. Failure of samples observed in chisel-test (manual destruction test)

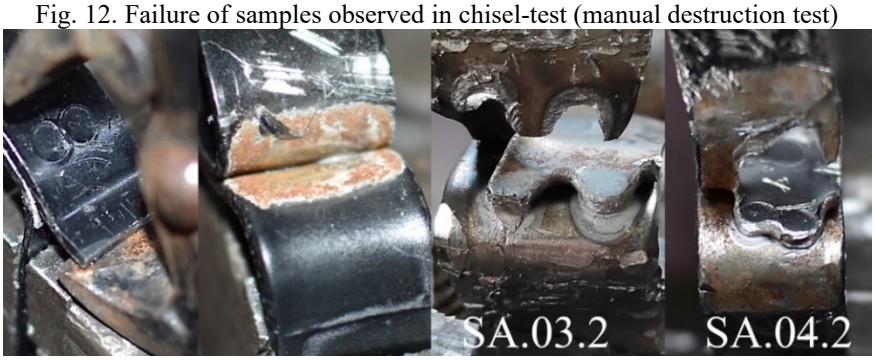

Fig. 13. Failure of samples observed in peel-test (manual destruction test)

Fig. 14. Failure of samples observed in chisel-test (manual destruction test)

During the simple test methods, the chisel test was performed on samples SA.02 andSA.06 (Fig.12 and Fig.14) and the peel test on the samples SA.03.2 and SA.04.2(Fig.13). These methods were difficult to be performed manually on the selected samples due to their high tensile resistance and thickness being evaluated also by mechanized tensile test. The result of the chisel test included the pull-out failure with sheets tearing for the sample SA.06. In this situation, the loading material was an axial tension (perpendicular load on the weld surface) in the middle of two welded spots which explains the breaking failure from inside-out (Fig.14). For the sample SA.02, in normal condition, with chisel on either side of the weld, only a nugget elongation (plastic deformation) without a material break was obtained (Fig.12). The welding spot mechanical characteristic was considerable increased in this situation. As for the peel test, using pliers by gripping the samples (SA.03.2, SA.04.2) in the vise, the crop of material was obtained around the welding spot (Fig.13). This indicates a good quality of the welded spot. By performing these tests, it was possible to observe the high load capacity of the tested samples with low ductility. The values obtained for the weld diameter were between 2.07 mm and 6.30 mm. To be suitable for functional use, depending on the operating conditions, the welding spot diameter must be above the minimum accepted value, according to the welding procedures and factory operating instructions.

4. Conclusions

Destructive testing on real structures revealed failure behaviour that was identical to that predicted theoretically (Fig.3), depending on the values of the applied forces. Depending on the thickness of the components and the position or number of welding spots, the breaking mode for the studied samples varied. In the case of several spot welds, the failure sequence was investigated, and it was discovered that their diameter and arrangement in relation to the part's axis is critical in ensuring the welded structure's load-bearing capacity. Deforming the area surrounding the welded point, where the material's plasticity is highest, is usually the most preferred method of yielding.

In contrast to previous studies [9–13] based on test circumstances in accordance with the standards EN ISO 5182:2016, the real destruction behaviour of these structures constructed under industrial conditions with various sheet thicknesses and distances between welding spots was highlighted through these

investigations. By plotting the load-displacement diagram, it was observed in the sheets with multiple welds the order of spots failure in relation with maximum value and direction of applied force at which the weld yields. Through these parameters, the geometry of the structures used can be optimized, by resizing the sheets, such as the use of thinner layers or a smaller number of welded points that can reduce working time and implicitly production costs. The laboratory tests carried out complement the industrial tests through which the breaking mode can only be qualitatively validated without being able to accurately establish the maximum forces to which the mechanical structures can be subjected. Within the tested structures (structures SA.01 and SA.02) it was also possible to observe the weak areas depending on the method of attachment and force actuation.

The welding parameters must be set in such a manner that the "failure to extract spot welding" mode is guaranteed. Pull failure was detected during manual tests in which axial forces were applied to the welds. Even though the mechanical fracture-shear tests produced extremely high load values (more than 31 kN for sample SA.01 and more than 26 kN for sample SA.05), only the interfacial fracture mode was seen for each sample examined. There was also evidence of the various welding points gradually failing.

Acknowledgements

The authors are grateful to S.C. SILDVB COM S.A, Romania for donating the industrial steel-sheets multiple welded spots with different thicknesses and geometries.

REFERENCES

[1] *Nielson K L and Tvergaard V,* Ductile Shear failure or plug failure of spot welds modelled by Gurson model, Engineering Fracture Mechanics, 77, 2010**.**

[2] *Zhang W, Jensen HH and Bay N,* Finite Element Modeling of Spot Welding Similar and Dissimilar Metals, 7th international conference on computer technology in welding, San Francisco: NIST Special Publication, pp 364-73, 1997.

[3] *Hasanbasoglu A and Kaçar R* Microstructure and property relationships in resistance spot weld between 7114 interstitial free steel and 304 austenitic stainless steel, J Mater Sci Technol, 22, 375, 2006.

[4] *Akkas N, Ilhan E, Varol F and Aslanlar S*, Welding time effect on mechanical proprietis resistance spot welding of S235Jr(Cu) steel sheets used in railway vehicles, ACta physica polonica A 129, 201, 2016.

[5] *Vural M and Akkus A*, On the resistance spot weldability of galvanized interstitial free steel sheets with austenitic stainless steel sheets, Journal of Materials Processing Technology 1, 2004.

[6] *Akkas N*, Effect of welding current and time on tensile-peel loading in resistance spot welding of SP-H steel sheets used in railway vehicles, Acta physica polonica A 132 no. 3, 2017.

[7] *Akkas N,* Welding time effect on tensile-shear loading in resistance spot welding of SP-H Weathering steel sheets used in railway vehicles, ACta physica polonica A 132 no. 1, 2017.

[8] *Thongchai Arunchai, Kawin Sonthipermpoon, Phisuit Apichayakul and Kreangsak Tamee,* Resistance Spot Welding Optimization Based on Artificial Neural Network, Hindawi Publishing Corporation International Journal of Manufacturing Engineering, 20, 2014.
[9] *Lin H L, Chou T and Chou C-P*, Optimation of resistance spot welding process using Taguchi method and a neural network, Experimental Techniques 31 no. 5, 2007.
[10] *Pouranvari M, Marashi P, Goodarzi M and Abedi A,* An analytical model predicting failure mode of resistance spot welds, Metal, Hradec nad Moravicí 5, 2008.
[11] *Sachin Patil and Hamid Lankarani,* Numerical Prediction of Various Failure Modes in Spotweld Steel Material, AE International Journal of Transportation Safety 6, 2018.
[12] *Pouranvi M and Marashi S.P.H,* Weld nugget formation and mechanical proprieties of three-sheet resistance spot welded low carbon steel, Canadian Metallurgical Quarterly 51, 2012.
[13] *Pouranvi M and Marashi S.P.H,* Critical review of automotive steels spot welding: process, structure and properties, Science and Technology of Welding and Joining 18, 2013.
[14] *Uncu I,* Research and Experimentation Regarding Destructive Test of Resistance Spot Welds Within Cushion Metal Frames of Automotive Seat Model Zafira (Brașov: PhD thesis), 2014.
[15] *Ungureanu D-V* , Cercetări Privind Sudarea Electrică prin Presiune în Puncte in Curent Continu a Tablelor Zincate, cu Implementare la Realizarea Subansamblelor de Tipul Grinzilor din Elemente Ușoare (Research regarding electric pressure spot welding in continuous current of galvanized sheets, with implementation in the realization of beam-type subassemblies from light elements), Timișoara, 2018 (In Romanian)
[16] *Stănoiu M-A,* Spot Welding of Sheets of Different Thicknesses, Identical Thicknesses, Screws and Nuts (University Politehnica of Bucharest: Master), 2020.
[17] Standards and Testing – Setting up a spot welding process: http://www.spottrack.eu/welcome/standards-testing.jsp, accessed at 02/2021
[18] BS EN ISO 10447 2015 Resistance Welding. Testing of Welds. Peel and Chisel Testing of Resistance Spot and Projection Welds.
[19] ISO 18595 2007(en) Resistance Welding –Spot Welding of Aluminium and Aluminium Alloys –Weldability, Welding and Testing.
[20] EN 1993-1-3 Eurocode 3 2006 Design of Steel Structures. Part 1-3: General Rules, Supplementary Rules for Cold-Formed thin Gauge Members and Sheeting (CEN, Brussels)
[21] ISO 5182 2016 Resistance Welding — Materials for Electrodes and Ancillary Equipment.
[22] Welding A. W. (2013). AWS D8.1 M: 2013 (American National Standard Specification for Automotive Weld Quality).